Proceedings of the ASME 2013 International Design Engineering Technical Conferences and Computers and Information in Engineering Conference
IDETC/CIE 2013
August 4-7, 2013, Portland, Oregon, USA

DETC2013-12503

MULTI-STAGE OPTIMIZATION OF WIND FARMS WITH LIMITING FACTORS

Bryony L. DuPont
Department of Mechanical Engineering
Carnegie Mellon University
Pittsburgh, PA 15232
bryony@cmu.edu

Jonathan Cagan
Department of Mechanical Engineering
Carnegie Mellon University
Pittsburgh, PA 15232
cagan@cmu.edu

ABSTRACT

Larger onshore wind farms are often installed in phases, with discrete smaller sub-farms being installed and becoming operational in succession until the farm as a whole is completed. An extended pattern search (EPS) algorithm that selects both local turbine position and geometry is presented that enables the installation of a complete farm in discrete stages, exploring optimality of both incremental sub-farm solutions and the completed project as a whole. The objective evaluation is the maximization of profit over the life of the farm, and the EPS uses modeling of cost based on an extensive cost analysis by the National Renewable Energy Laboratory (NREL). The EPS uses established wake modeling to calculate the power development of the farm, and allows for the consideration of multiple or overlapping wakes.

A limiting factor is used to determine the size of wind farm stages: optimization stages based on the number of turbines currently available for development (representative of limitations in initial capital, which is commonly encountered in wind farm stage development). Two wind test cases are considered: a unidirectional test case with constant wind speed and a single wind direction, and a multidirectional test case, with three wind speeds and a defined probability of occurrence for each. The test case shown in the current work is employed on a 4000 km by 4000 km solution space. In addition, two different methods are performed: the first uses the optimal layout of a complete farm and then systematically "removes" turbines to create smaller sub-farms; the second uses a weighted multi-objective optimization over sequential, adjacent land that concurrently optimizes each sub-farm and the complete farm. The exploration of these resulting layouts indicates the value of full-farm optimization (in addition to optimization of the individual stages) and gives insight into how to approach optimality in sub-farm stages. The behavior exhibited in these tests cases suggests a heuristic that can be employed by wind farm developers to ensure that multi-stage wind farms perform at their peak throughout their completion.

INTRODUCTION

As the United States seeks to diversify its energy portfolio and generate more power from domestic and renewable sources, wind power is poised to become a significant portion of the U.S. total energy supply [1]. In fact, the U.S. is currently ranked second in the world for new wind power capacity growth [2], though is still far from the high percentages of wind–derived power seen in many European countries. The United States Department of Energy has laid a course to generate 20% of the country's electricity using wind power by 2030 [1] . As of September 2012, The U.S. has installed just over 51 GW [3] of the 305GW required to meet this goal. In order to continue wind energy's growth and ensure that the country meets its rising electricity demand using renewable sources, it is imperative that the optimality of wind farms are considered from the first phases of planning.

Many new onshore wind farms in the Unites States are very large, such as the 390-turbine 1020 MW Alta Wind Energy Center in California [4], the 627-turbine 781.5 MW Roscoe Wind Farm in Texas [5], and the 421-turbine 735.5 MW Horse Hollow Wind Energy Center in Texas [6]. Each of these was built in multiple stages, that is, preliminary smaller wind farms were installed and integrated into the electricity grid, and subsequent sub-farms were then built on adjacent land until the entire project was completed. This creates an interesting layout problem from an engineering optimization perspective – the optimal layout for the completed farm is likely not simply the aggregate of the optimal layouts of the discrete sub-farms. This work seeks to explore the optimization of multi-stage wind farms, and gives suggestions for the best means of performing a priori optimization on real-world wind farms.

This multi-stage wind farm optimization is performed by building on the capabilities of an existing wind farm optimization algorithm, an extended pattern search (EPS) within a multi-agent system, developed by DuPont and Cagan [7]. In this paper, previous approaches to wind farm layout optimization, including the prior version of the EPS, are discussed. The methodology of the current extension of the EPS algorithm to accommodate sub-farm design is explored, followed by

Copyright © 2013 by ASME

Downloaded From: http://proceedings.asmedigitalcollection.asme.org/ on 03/27/2015 Terms of Use: http://asme.org/terms

an explanation of both problem formulations: the full-farm optimization with reduction, and the multi-objective optimization of both the sub-farms and the complete farm. Lastly, resulting wind farm layouts and turbine geometries will be shown, along with discussion of the results.

PREVIOUS WORK

Work in the computational optimization of wind farm layouts has been explored for many years, though significant advances have been made recently due to increasing computational capability and interest. The driving force influencing wind farm layout optimization is the fact that turbines that are placed in close proximity can experience power development deficits due to the decrease in wind speed caused by the rotating blades of neighboring (upstream) turbines. While generally the addition of more turbines to a site will allow for the generation of more power, one must consider potential array losses (the reduction of energy development) in determining the local positioning of each turbine [8].

Of the varying computational algorithms applied to wind farm layout optimization, genetic algorithm (GA) approaches have been the most popular. The first of these, by Mosetti et al. [9], established the test scenario that has been repeatedly employed for comparison purposes. This test case is a square 2 km x 2 km field, depicting an aerial view of turbines on a 2-D discretized solution space. Mosetti et al.'s GA used an objective function that maximized the power development of the farm while minimizing an estimation of the normalized cost, and employed wake modeling developed by Jensen [10] to determine the effective wind speed at each turbine. Grady et al. [11] introduced a GA that improved upon Mosetti et al.'s method by utilizing advanced computational resources.

Multiple researchers have developed GA's that expand upon the performance of these preliminary works. Multiple reports by Elkington et al. [12,13] suggest that Genetic Algorithms are best suited for offshore wind optimization. Wan et al. [14] utilized the same discretized solution space as previous researchers, but applied more accurate modeling of power. Wang et al. used grid-placement techniques in conjunction with a GA [15], and employed non-linear wake expansion to estimate the effects of wakes [16]. Huang used a distributed GA (DGA), which divided large populations into smaller populations for computational efficiency [17], and later combined this DGA with a gradient search method to produce more optimal layouts [18]. Sisbot et al. [19] applied a multi-objective GA to a realistic potential wind site, using advanced cost modeling, while Emami et al. [20] also used a weighted multi-objective GA to explore the trade-off between wind farm power development and cost. Rasuo et al. [21] explored the application of a GA to wind farms on varied terrain, which captured real-world topographical challenges in wind farm micrositing.

In addition to genetic algorithms, multiple other methods have been used to solve the wind farm layout optimization problem. Ozturk et al. [22] used a heuristic method to place turbines, while Bilbao et al. [23] employed a simulated annealing algorithm. Muskaterov et al. [24] developed a mixed-integer nonlinear discrete combinatorial optimization algorithm that employed both a square and rectangular solutions space, which influenced the use of those shapes in the solutions spaces of the current work. Wan et al. [25] expanded on their previous GA approach by creating a particle swarm optimization (PSO) approach. The methodology on which the current work is based, an Extended Pattern Search, has also been successfully applied to wind farm layout optimization and has incorporated multiple advances in modeling that enable the development of more real-world applicable wind farm layouts [7,26].

There are several recent works the seek to expand on the capability of various algorithms such that state-of-the-art modeling of cost, wake interaction, and power are incorporated into the optimization. Zhang et al. [27] created a cost surface to more accurately estimate the costs associated with wind farm development. Chowdhury et al. [28] established a framework for the selection of turbines with varying rotor radii, and DuPont et al. [26] expanded the capability of their EPS algorithm to select both turbine hub heights and rotor radii. Bentatiallah et al. [29] used actual long-term wind data as an input to their genetic algorithm for wind farm layout. Chen et al. [30] explored the implications of landowner decisions on resulting farm layouts. Kusiak et al. [31] used preliminary data mining in conjunction with a GA to determine the optimal control settings for a proposed farm. More recent work by Chowdhury et al. [32] used a Kernel Density Estimation to better model multi-modal wind data. These advances suggest that it is not only the choice and development of the optimization algorithm itself, but also the advances in how wind farm optimization is modeled that will lead to robust and thoroughly tested proposed layouts that perform as predicted.

In keeping with the current trend to advance both modeling and algorithm capability, the current work establishes the means to develop wind farms in stages, such that optimality is considered during both sub-farm and complete farm implementation. The EPS within a multi-agent system [26] is used as the basis for the optimization, as it is designed to select both turbine placement and geometry, account for variation in atmospheric stability conditions and wind shear profile shape, incorporate the effects of partial wake interaction. The EPS/MAS has previously developed superior layouts than comparable algorithms on traditional test cases.

Previous literature suggests there is need for the exploration of the incremental optimization of wind farms. An empirical analysis of existing multi-stage U.S. wind farms shows that stages generally include an estimated 50-150 turbines. These stages combine with other stages to establish preliminary sub-farms, and eventually very large completed farms. Sub-farms become operational while subsequent stages are still being constructed, providing power to the grid and essentially functioning as discrete entities. Additional stages tend to be on adjacent or nearby plots of land, and often exhibit the placement of turbines in straight lines to benefit from a predominant wind direction (such as the 222 MW, three-stage Stateline Wind Project in Oregon [33]). Many relevant research questions arise from studying wind farms built in stages. Primarily, we seek to understand the trade-off in performance when considering optimal sub-farm layouts and/or optimal complete farm layouts, and to discover any potential heuristics that can be applied to improve multi-stage wind farm layout in the future.

EPS METHODOLOGY

An Extended Pattern Search algorithm advances the traditional deterministic pattern search algorithm in that it includes stochastic elements (called "extensions") to facilitate escaping inferior local optima. Driven by its successful application to other complex layout problems [34], EPS has previously been applied to wind farm layout optimization, producing superior results than comparable genetic algorithm approaches [7]. A traditional pattern search traverses a user-defined set of pattern directions (in this case, +y, -x, -y, +x) at a given step size, testing the objective function evaluation at each potential move. A move is only selected if it benefits the evaluation, and if not potential moves are chosen at a given step size. Once there is no further benefit, the step size is reduced and the search is repeated. This deterministic behavior lends to certain convergence, but global optimality is not guaranteed (or in some formulations, even likely).

 Copyright © 2013 by ASME

Downloaded From: http://proceedings.asmedigitalcollection.asme.org/ on 03/27/2015 Terms of Use: http://asme.org/terms

Therefore, to enable the search to escape local optima, three stochastic extensions are employed: 1) an initial random layout removes any bias that may come about by a user-defined initial placement, 2) the search order through which the algorithm determines turbines to move is randomized such that no turbine's movement is favored, and 3) a "popping" algorithm that selects poorly-performing turbines based on power development attempts to relocate these turbines to random locations, only allowing the move if it benefits the global evaluation.

The EPS for turbine layout also includes two sub-level EPS algorithms that select both turbine hub height and rotor radius, constraining the relationship between the two such that infeasible designs are not considered. This enables the search to not only move turbines such that they avoid being placed in the wakes of upstream turbines, but to also select turbine geometry that can help avoid wake interaction and maximize individual turbine power development. The pattern directions for these searches (as shown in Figure 1) are +l, -l, +l/2, and –l/2, where l is the height and the radius, respectively.

The EPS is employed within a multi-agent system, primarily to facilitate changes to the algorithm as advances in modeling are made. The software agents of a multi-agent system work individually to meet their own goals, but if enabled to communicate within other agents, a multi-agent system can collectively work towards a balance between the global optimum and their individual objectives. In this multi-agent system, each turbine is an individual software agent, capable of retaining information about itself and its neighbors. Multi-agent system strategies have been very successful when applied to engineering design problems, such as A-Teams[35], A-Design [36], and blackboard systems [37].

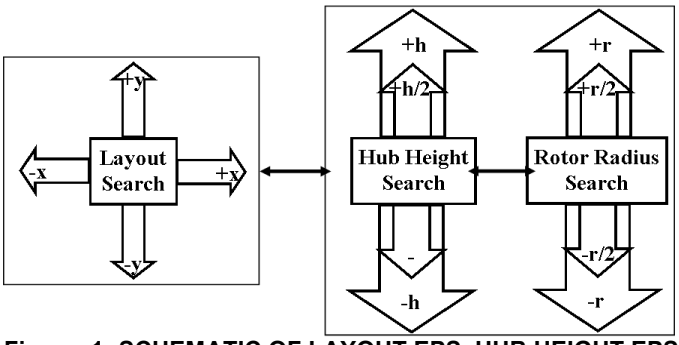

Figure. 1: SCHEMATIC OF LAYOUT EPS, HUB HEIGHT EPS, AND ROTOR RADIUS EPS

In addition, the EPS incorporates local information about the potential farm site's atmospheric stability conditions to more accurately predict the power development of the farm. In the atmospheric boundary layer – the region of air closest to the earth's surface – variation in temperature, local wind direction, humidity, air density, and other parameters often occur due to changes in atmospheric stability. Stability is traditionally classified as being stable, unstable, or neutral, and is dependent on the relationship between the temperature of the air and the temperature of the earth's surface, such that stability conditions cycle throughout the day. Unstable atmospheric conditions occur when warmer air is situated below cooler air (as is the case when the earth's surface is warmed by the sun), which can cause significant mixing that affects wind flow and temperature gradients [38], leading to flow conditions which can cause early rotor fatigue over time [39]. It is important to account for these effects as it is established that atmospheric stability affects wind farm performance [40], with research pointing to a 5% overestimation of the wind capacity of a site due to neglecting the consideration of atmospheric stability [41]. For simplification, the current work uses site-averaged neutral atmospheric condition parameters derived from the Lamar Low Level Jet (LLLJP) data [42].

The atmospheric stability of the site is considered in two ways. First, the power law is applied to account for variation in wind speed with respect to height, representative of boundary layer flow principles. The power law is governed by Eq. (0) [8]:

$$U(z) = U(z_r)\left(\frac{z}{z_r}\right)^{\alpha_h}, \tag{0}$$

where $U(z)$ is the wind speed with respect to height z, $U(z_r)$ is the reference wind speed at reference height z_r,, and α_h is the power law exponent. The power law exponent α_h varies with changes in atmospheric stability conditions, and is estimated by averaging yearly wind shear exponent data from the Lamar Low-Level Jet Program (LLLJP) [42]. Based on extensive wind data from the site near Lamar, Colorado, USA, the yearly averaged power law exponent for heights of 3 meters to 113 meters is $\alpha_h = 0.15567$.

The second means through which atmospheric stability is considered is through variation of the wake decay constant. The wake decay constant plays a role in determining how far downstream the wind speed within a wake recovers, as well as helping to determine the width of downstream wakes (as formulated in Eq. (3) and Eq. (5) As such, variation in the wake decay constant due to atmospheric stability can have a significant effect on the power development of wind turbines. In general, the more stable the atmosphere, the lower the wake decay constant [43], and it has been suggested that most approaches fail to accurately estimate the wake decay constant, particularly for unstable conditions [44–46]. In this work, we model the wake decay constant as a function of height, derived from the turbulence intensity of the Lamar Low Level Jet Program site [42]. This estimation allows us to understand how changes in atmospheric stability relatively affect optimal layouts and turbine geometry as conditions would change between potential sites. The formulation for the wake decay constant for neutral conditions is stated in Eq. (1):

$$k(h) = 0.088h^{-0.152}. \tag{1}$$

MODELING

A). Wake Model and Partial Wake Interaction

The flow behind rotating turbine blades is complex and difficult to capture without incurring significant computational cost, so the need to formulaically model downstream airflow is paramount in highly iterative algorithms like EPS. The EPS algorithm employed in this work utilizes a 3-D extrapolation of the PARK wake model [10] to estimate the effect that a wind turbine has on the air flow directly downstream of its rotor. This wake is assumed to be conical in shape (as shown in Figure 2) wherein the wind speed is significantly reduced just behind the rotor but continually gains speed and asymptotically approaches the oncoming wind speed as the wake traverses downstream distance. Mathematically, both the width of the downstream wake and the wind speed deficit are proportional to the distance downstream from the rotor, as stated in the momentum balance given in Eq. (2):

Copyright © 2013 by ASME

Downloaded From: http://proceedings.asmedigitalcollection.asme.org/ on 03/27/2015 Terms of Use: http://asme.org/terms

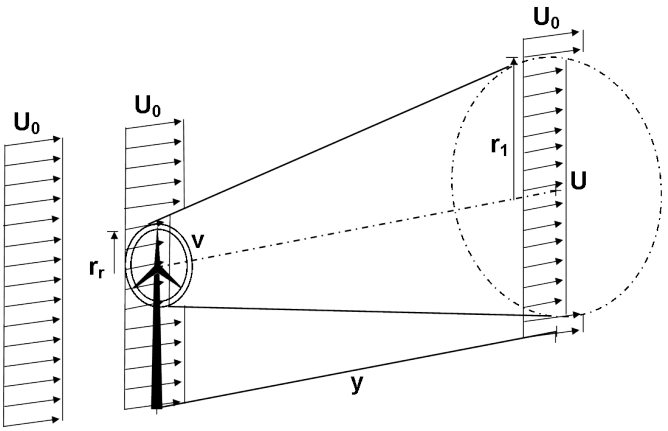

Figure 2: DEPICTION OF FRUSTUM-SHAPED 3-D WAKE

$$\pi r_r^2 v + \pi\left(r_1^2 - r_r^2\right)U_0 = \pi r_1^2 U. \qquad (2)$$

In Eq. (2), U_0 is the ambient wind speed, r_r is the radius of the turbine rotor, r_1 is the radial width of the wake at distance x downstream from the turbine, v is the velocity directly behind the turbine (approximately 1/3 of the ambient wind speed), and U is the wind speed within the wake at distance downstream. U is a decremented representation of U_0 and is abstracted to be constant across the cross-section of the wake. The formula for U, the downstream wind speed within the wake, is given by:

$$U = U_0\left(1 - \frac{2}{3}\left(\frac{r_r}{r_r + ky}\right)^2\right). \qquad (3)$$

A turbine that is placed such that it does not incur any wake effects from upstream turbines has an effective wind speed equivalent to the unobstructed ambient wind speed approaching the farm. To determine the effective wind speed for any turbine that lies within a single wake, Eq. (3) is used, where k is the wake decay constant, the formula for which is given in Eq. (1) for the neutral atmospheric stability case. To calculate the effective wind speed for a turbine placed in multiple wakes, the individual kinetic energy losses caused by each of the n wakes must be summed using Eq. (4):

$$U = U_0\left[1 - \sqrt{\sum_{i=1}^{n}\left(1 - \frac{U_i}{U_0}\right)^2}\right]. \qquad (4)$$

At each iteration, the turbine agents must determine which turbines are upstream and creating a wake, and which turbines it in turn affects downstream. A rectangular neighborhood in (x,y) is used to preliminarily determine which turbines have wake interactions, using Eq. (5) to determine the width of the wake at a given distance:

$$r_1 = r_r + ky\,. \qquad (5)$$

Using these rectangular neighborhoods, each rotor's frustum shaped wake is established to determine the percentage of the rotor swept area of downstream turbines that lie within that wake. Three distinct partial wake interaction scenarios are considered [26]. The first is a turbine rotor that is partially located within the wake of one upstream turbine, or two upstream turbines whose wakes do not overlap across the rotor swept area, such that each percentage of overlap can be calculated individually. The second is the case of multiple wakes that overlap across a turbine's rotor swept area, which necessitates a discretization of the rotor swept area in order to estimate the combinatory effects of the overlapping portions of the wakes. The third scenario, which is unlikely due to wake expansion during propagation, is when the entire cross-section of a wake lies within the rotor swept area of a downstream turbine; the percentage of overlap in this case can be calculated directly.

The use of the PARK wake model is imperative to ensure the efficient computational time of the EPS algorithm, but it does simplify the usually complex wake behavior created by rotating turbine blades. Primarily, the wind speed within a wake is considered constant across the cross-section, and exhibits binary behavior at the wake boundary that would be more accurately represented by a wind speed gradient [47]. The model also lacks the capability to capture the complex wake behavior directly behind a rotor, though the minimum-distance requirement between turbines is large enough to ensure that turbines are not placed in these difficult portions of the wakes. The current work extrapolates this model to 3-D and allows for partial wake interaction, which is nonetheless an improvement over previous applications of the PARK wake model.

B) Power Modeling

An estimation of the power development of a single turbine is given in Eq. (6) [8]:

$$P = \frac{1}{2}\rho A U^3 C_P\,, \qquad (6)$$

where ρ is the density of air (considered constant at 1.225 kg/m^3), A is the cross-sectional area swept by the rotor blades, U is the effective wind speed, and C_p is the power coefficient. Additionally, to mimic the power curves of commercially available turbines, a rated wind speed of 11.5 m/s is enforced, such that at wind speeds higher than the rated wind speed, a turbine will only produce the amount of power it would at 11.5 m/s. The turbine will not produce power at wind speeds below the cut-in speed of 3 m/s. The total power output of the farm is considered to be the sum of the individual power developments of each turbine.

C) Cost Modeling

Similar to the cost model explored in previous work [26], the National Renewable Energy Laboratory's Wind Cost and Scaling Model [48] was used to create a more realistic prediction of the costs associated with installing a wind farm. The total estimation of cost contains many factors, such as the land lease costs for the farm site, the materials and manufacturing costs for turbine production, and the operation and maintenance costs of the farm. To facilitate wind farm developers and researchers, the NREL cost model is integrated into a freely-available spreadsheet, called the Jobs and Economic Development Impact (JEDI) model for wind [49] that was used to develop the cost surface employed in this work. A matrix of feasible turbine geometries was developed along with the resulting predicted power development of each combination of hub height and rotor radius. This matrix was then used as an input to the JEDI spreadsheet, which created an estimation of cost based on hub height and rotor

Copyright © 2013 by ASME

Downloaded From: http://proceedings.asmedigitalcollection.asme.org/ on 03/27/2015 Terms of Use: http://asme.org/terms

radius. The cost surface for neutral stability conditions is pictured in Figure 3:

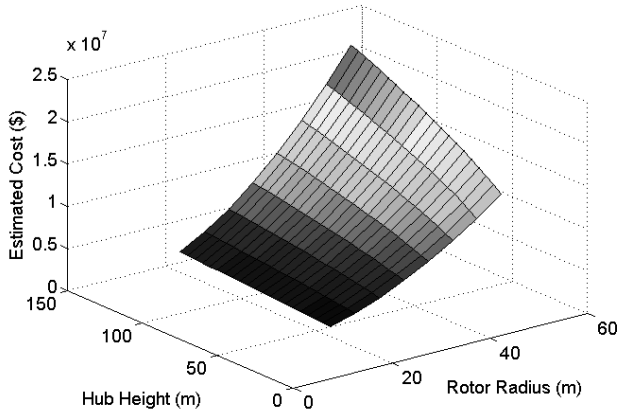

Figure 3: COST SURFACE DEVELOPED FROM NREL JEDI SPREADSHEET (NEUTRAL STABILITY CONDITIONS)

The cost as a function of hub height and rotor radius for neutral stability conditions is given in Eq. (7):

$$Cost(h,r) = (2.454e+06) - (2.161e+05)r + (1.203e+04)h + 6039r^2 + 2455rh - 161.2h^2 \quad (7)$$

D) Objective Function

The objective function used for evaluation throughout the EPS run is that of the maximization of profit over a set farm lifetime. To conform to traditional negative null form, the objective function considered here is the minimization of negative profit. Once the total power development of the farm and the total cost (the sum of the individual turbine costs) are calculated, the objective function can be evaluated:

$$Objective = Cost_{\text{Project}} + \left(Cost_{O\&M} \times t\right) - \left(Energy_{Yearly} \times C_F \times t \times COE\right), \quad (8)$$

where C_F is the capacity factor, and COE is the cost of energy – the price at which a farm owner may sell the energy their farm develops, in \$/kWh, and t is the life of the farm in years. $Cost_{Project}$ is the cost that is estimated using the cost surface formula in Eq. (7). $Cost_{O\&M}$ is the annual operations and maintenance cost of the farm in \$/year, and is given by [48]:

$$Cost_{O\&M} = 0.007 \times Energy_{Yearly} \times C_F \times COE. \quad (9)$$

The life of each turbine is considered to be 20 years, irrespective of its stage. Future work will consider the life of the farm as a whole, and how having earlier turbines have that longer relative lives affects the optimization.

PROBLEM FORMULATION

The EPS is applied to a test solution space, a square 4 km x 4 km field, as depicted in Figure 4.

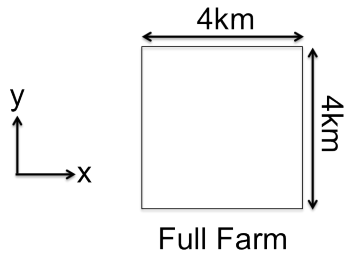

Figure 4: SQUARE SOLUTION SPACE

Two test cases are presented. The first test wind case is that of constant, unidirectional wind (representing the prevailing wind direction on a theoretical farm), from the bottom of the field upward in the positive-Y direction at 10 m/s. The second test wind case is multidirectional, considering 36 wind directions (in increments of ten), three wind speeds (8, 12, and 17 m/s), with a probability of occurrence for each, as depicted in the bar graph in Figure 5.

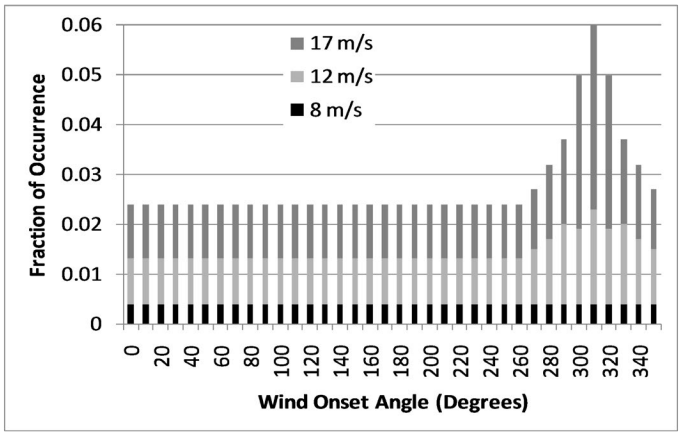

Figure 5: MULTIDIRECTIONAL WIND TEST CASE, PROBABILITY OF OCCURRENCE FOR EACH WIND SPEED AND WIND DIRECTION

Two methodologies are presented. First, The "full-farm" optimization (Figure 4), in which the complete field of 40 turbines is optimized using the EPS algorithm, and sub-farms are created by "removing" turbine stages from within the full solution space. The second method, the multi-objective optimization case (Figure 6), consists of each stage being assigned to adjacent plots of land (imitating the successive development of many current multi-stage wind farms). The full-farm optimization does not restrict the internal placement of turbines aside from a minimum distance requirement, while the multi-objective optimization additionally constrains turbine placement to a set number of turbines (representative of fixed capital) in each adjacent stage. In both methods of wind farm optimization in stages both the square and rectangular solution spaces are employed. Though multi-stage wind farms tend to be very large, to spare computational expense the current work explores a completed wind farm of 40 turbines, with stages being added in increments of 10.

Copyright © 2013 by ASME

Downloaded From: http://proceedings.asmedigitalcollection.asme.org/ on 03/27/2015 Terms of Use: http://asme.org/terms

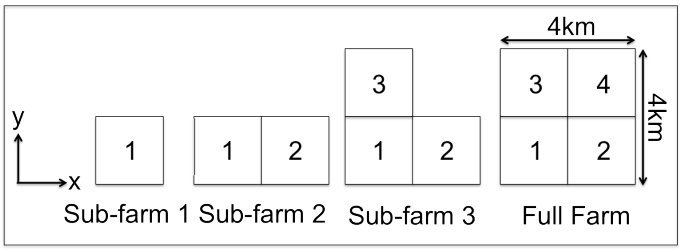

Figure 6: 4 km x 4 km SQUARE FIELD FOR MULTI-OBJECTIVE OPTIMIZATION

A) Full-Farm Optimization

The preliminary means of optimizing wind farm development in stages is to approach the problem as if the optimization of the complete, finished farm is the goal. The full farm is optimized, then turbines will be systematically "removed" from the completed layout to meet either the specified number of turbines to be placed on each sub-farm or the cost associated with the development of each sub-farm. This approach differs from traditional wind farm staging in that we explore the addition of stages to the existing solution space, without constraining the internal placement to assigned stages, instead of using adjacent land. The EPS within a multi-agent system creates an optimal layout of 40 turbines, and for each stage turbines are removed such that the global objective evaluation is the least impacted. That is, starting with 40 optimally placed turbines, each turbine will be removed individually and the global objective evaluation calculated for each removal, and the turbine that has the least impact on the global objective evaluation is removed. This process is computationally expensive, creating a large tree structure, one branch of which is depicted in Figure 7.

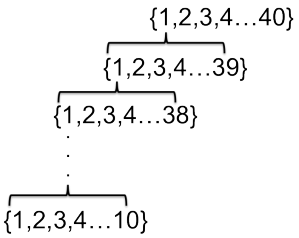

Figure 7: SINGLE BRANCH OFTREE STRUCTURE GENERATED BY REMOVAL OF INDIVIDUAL TURBINES

To determine which turbines should be removed for each stage without completing a costly exhaustive search of the large solution tree, a genetic algorithm was employed to aid in selecting the appropriate turbines for each sub-farm. The search uses the hierarchy depicted in Figure 8.

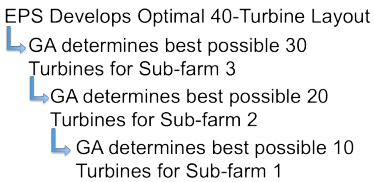

Figure 8: HEIRARCHY FOR FULL-FARM OPTIMIZATION APPROACH

The genetic algorithm used to search the solution tree is based on the micro-GA work of Senecal [50], where the "micro" designation implies there are a relatively small number of parent strings. First, the EPS/MAS system develops ten optimal layouts for the number of turbines to be utilized in the completed farm (for this test case, 40 turbines), and the best of these is chosen. With the final farm positions and turbine geometries selected, a GA is employed to determine which of the 40 turbines will be included at each state of the farm's development. The GA consists of parent strings that indicate whether or not a turbine exists in the optimal EPS/MAS-derived layout. The objective function evaluation between parents compares the potential profit (as given in Eq. (8)) for a farm whose included turbines are defined by the parent string. For the full layout of 40 turbines, a set number (in this case, a stage of 10) of turbines are removed from the parent strings, such that the solution includes just the number of turbines for the next-smallest-sized sub-farm. After the sub-farm of 30 is generated, the process repeats to develop the sub-farm of 20, and so on. The best EPS result out of ten are selected, then the GA are performed ten times, using 100 parent strings and 15k iterations, and converged to the same result every trial. The GA method is described in Figure 9.

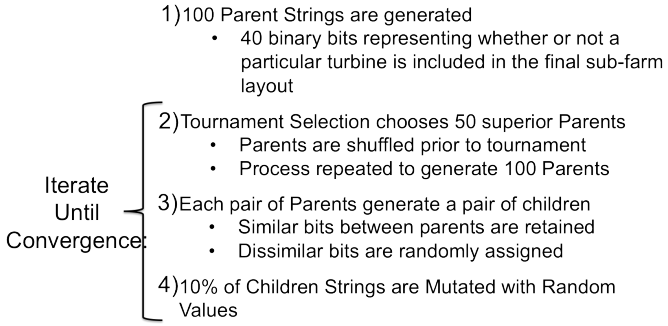

Figure 9: PSEUDO-CODE FOR GENETIC ALGORITHM FOR TREE SEARCH, FULL FARM OPTIMIZATION

B) Weighted Multi-Objective Optimization Over Sequential, Adjacent Land

A second approach to wind farm layout optimization in stages is the use of a weighted multi-objective optimization. In this test case, each stage is installed on separate land (divided into sub-farms as depicted in Figure 6.). This method employs a multi-objective optimization, where the objective function evaluation consists of both the individual evaluations of each sub-farm and the evaluation of the full farm. Each of these objectives has an associated user-defined weighting factor that determines the percent at which each evaluation will contribute to the global objective, as formulated in Eq. (10):

$$Objective = w_1 obj_{sub-farm1} + w_1 obj_{sub-farm2} + w_1 obj_{sub-farm3} + w_2 obj_{full\ farm} \quad (10)$$

The weighted multi-objective optimization seeks to explore the trade-off between optimizing the sub-farms (as they are operational years prior to the completion of the farm) and optimizing the full-farm layout. As a preliminary exploration of the trade off between sub-farm and full-farm objectives, each weighting factor is initialized to 25%, meaning that each sub-farm has the same weighting. Each of the four stages is restricted to contain only 10 turbines, which constrains the layout to represent building stages on adjacent land.

Copyright © 2013 by ASME

Downloaded From: http://proceedings.asmedigitalcollection.asme.org/ on 03/27/2015 Terms of Use: http://asme.org/terms

RESULTS

Images depicting the final layouts and turbine geometries for the square test case are presented, with quantitative results given in corresponding tables. A minimum distance requirement is enforced to ensure that turbines are not placed too close together. A legend that designates the symbols that represent the resulting ranges of the hub heights and rotor radii is given in Figure 10.

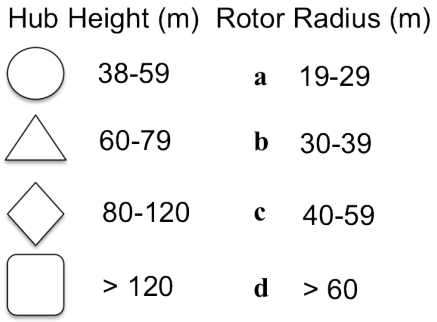

Figure 10: LEGEND FOR TURBINE GEOMETRY SYMBOLS

A) Unidirectional Case, Full-Farm Optimization

TABLE 1: RESULTS FOR FULL-FARM OPTIMIZATION, 10 - 40 TURBINES, SQUARE FIELD, UNIDIRECTIONAL CASE

N	Objective	Power (MW)	Avg. Hub Height (m)	Avg. Rotor Radius (m)
40	-1.23E+08	150	111.31	52.46
30	-1.11E+08	139	126.69	59.85
20	-7.94E+07	109	134.77	65.85
10	-4.42E+07	55.9	134.77	66.35

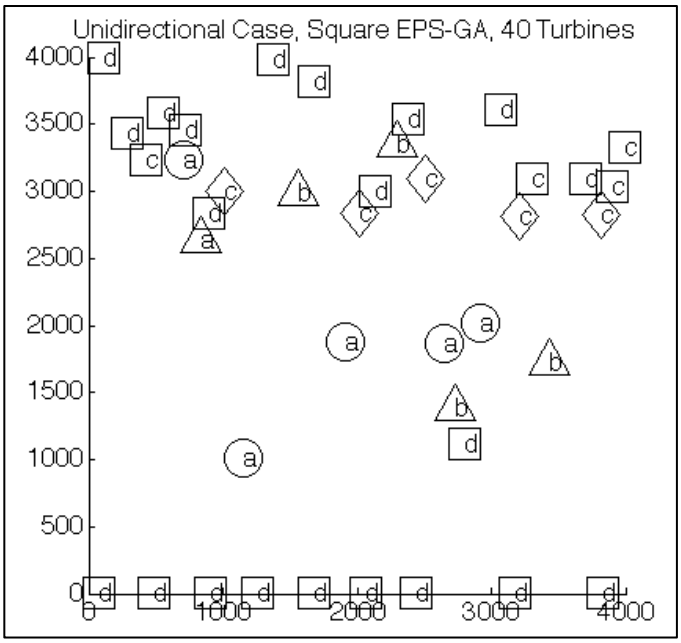

Figure 11: FULL-FARM OPTIMIZATION, SQUARE FIELD, 40 TURBINE COMPLETE FARM

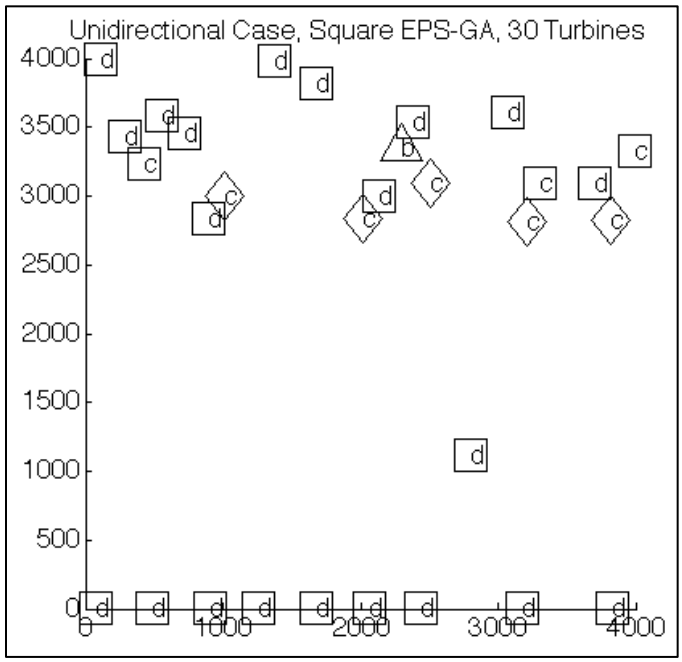

Figure 12: FULL-FARM OPTIMIZATION, SQUARE FIELD, 30 TURBINE SUB-FARM

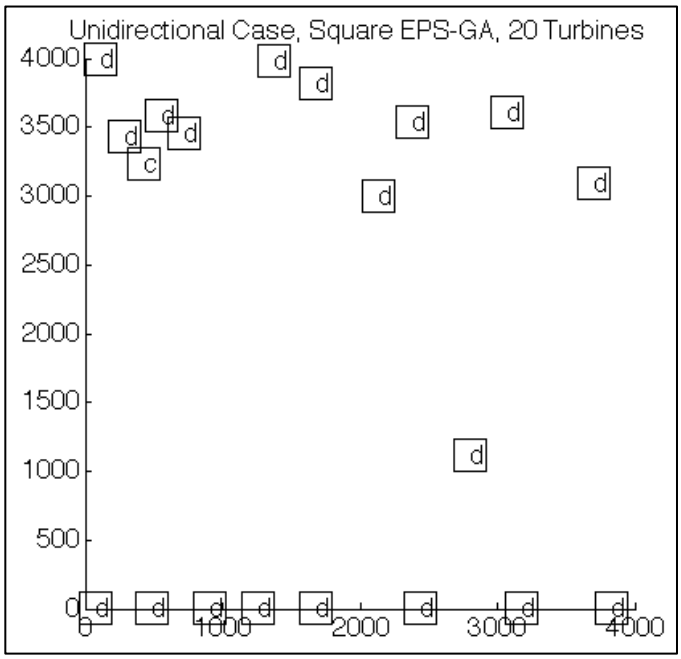

Figure 13: FULL-FARM OPTIMIZATION, SQUARE FIELD, 20 TURBINE SUB-FARM

Copyright © 2013 by ASME

Downloaded From: http://proceedings.asmedigitalcollection.asme.org/ on 03/27/2015 Terms of Use: http://asme.org/terms

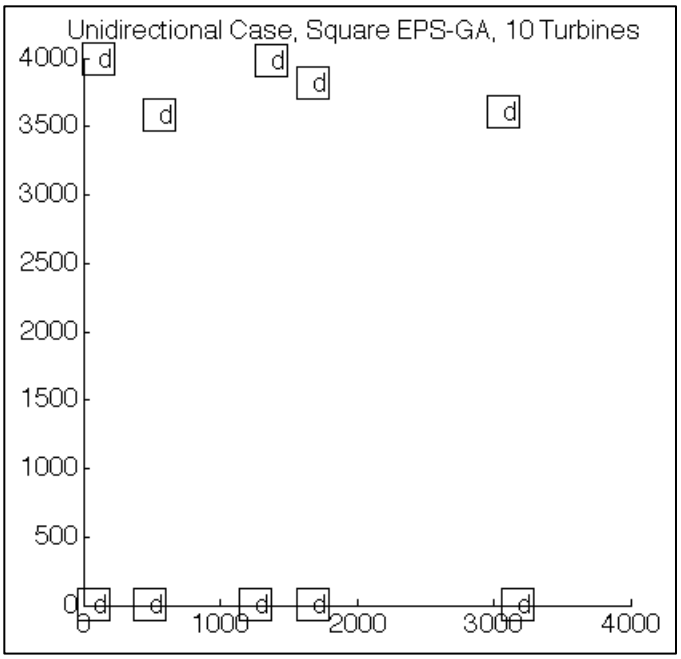

Figure 14: FULL-FARM OPTIMIZATION, SQUARE FIELD, 20 TURBINE SUB-FARM

B. *Unidirectional Case, Multi-Objective Optimization Over Sequential, Adjacent Land*

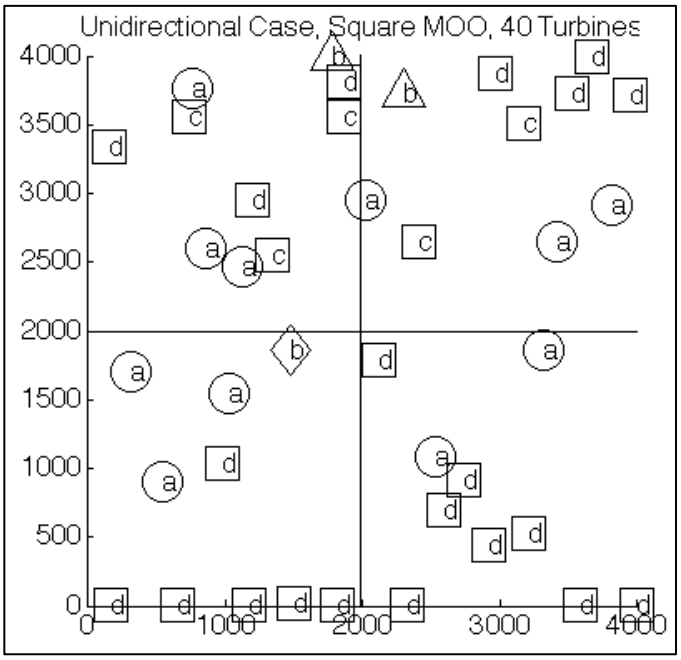

Figure 15: UNIDIRECTIONAL CASE, MULTI-OBJECTIVE OPTIMIZATION OVER SEQUENTIAL LAND, SQUARE FIELD, 40 TURBINES

TABLE 2: MULTI-OBJECTIVE OPTIMIZATION RESULTS, 40 TURBINES, SQUARE FIELD, UNIDIRECTIONAL CASE

N	Objective	Power (MW)	Avg. Hub Height (m)	Avg. Rotor Radius (m)
40	-9.15E+07	146	106.60	50.68
30		113	109.30	52.09
20		82	119.02	57.48
10		36.7	107.91	51.75

C) *Multidirectional Case, Full Farm Optimization*

Table 3: RESULTS FOR FULL-FARM OPTIMIZATION, 10 - 40 TURBINES, SQUARE FIELD, MULTIDIRECTIONAL CASE

N	Objective	Power (MW)	Avg. Hub Height (m)	Avg. Rotor Radius (m)
40	-1.53767e+08	125.77	100.32	49.91
30	-7.90587e+07	104.62	101.61	50.54
20	-7.593e+07	77.46	105.63	52.61
10	-4.32184e+07	40.87	107.98	53.82

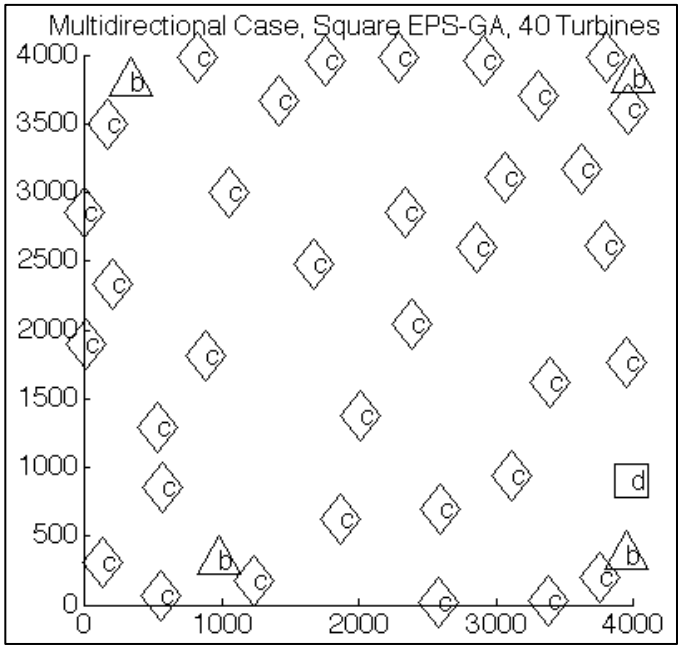

Figure 16: MULTIDIRECTIONAL CASE, FULL-FARM OPTIMIZATION, SQUARE FIELD, 40 TURBINES

Copyright © 2013 by ASME

Downloaded From: http://proceedings.asmedigitalcollection.asme.org/ on 03/27/2015 Terms of Use: http://asme.org/terms

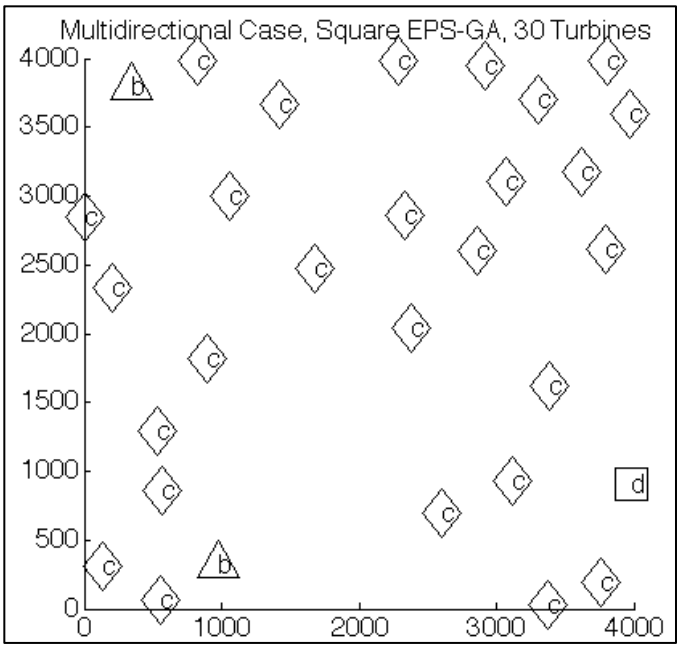

Figure 17: MULTIDIRECTIONAL CASE, FULL-FARM OPTIMIZATION, SQUARE FIELD, 30 TURBINES

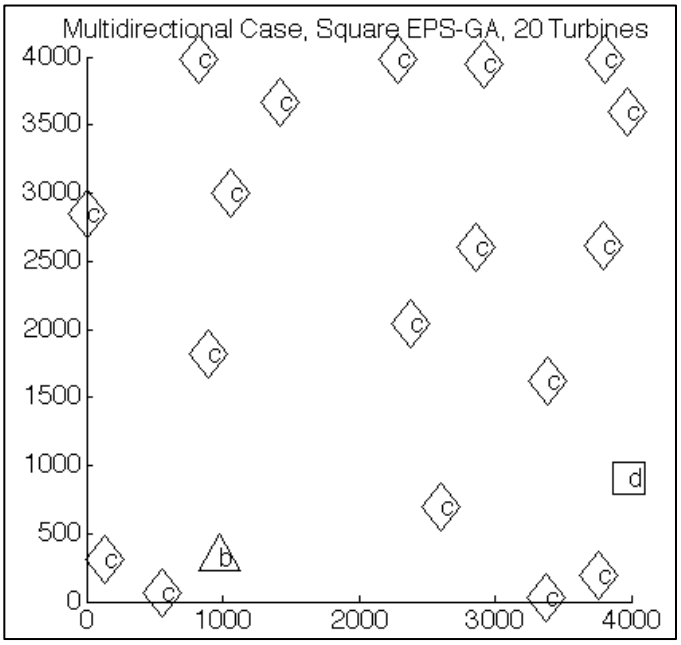

Figure 18: MULTIDIRECTIONAL CASE, FULL-FARM OPTIMIZATION, SQUARE FIELD, 20 TURBINES

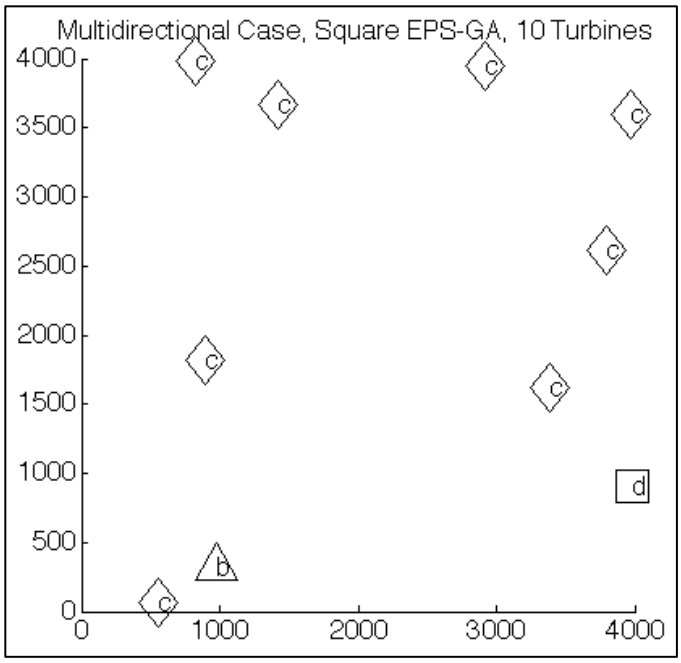

Figure 19: MULTIDIRECTIONAL CASE, FULL-FARM OPTIMIZATION, SQUARE FIELD, 10 TURBINES

D) *Multidirectional Case, Multi-Objective Optimization Over Sequential Stages*

Table 4: MULTI-OBJECTIVE OPTIMIZATION RESULTS, 40 TURBINES, SQUARE FIELD, UNIDIRECTIONAL CASE

N	Objective	Power (MW)	Avg. Hub Height (m)	Avg. Rotor Radius (m)
40	-8.78463e+08	217.83	134.81	66.90
30			134.84	66.91
20			134.84	66.91
10			134.84	66.91

Copyright © 2013 by ASME

Downloaded From: http://proceedings.asmedigitalcollection.asme.org/ on 03/27/2015 Terms of Use: http://asme.org/terms

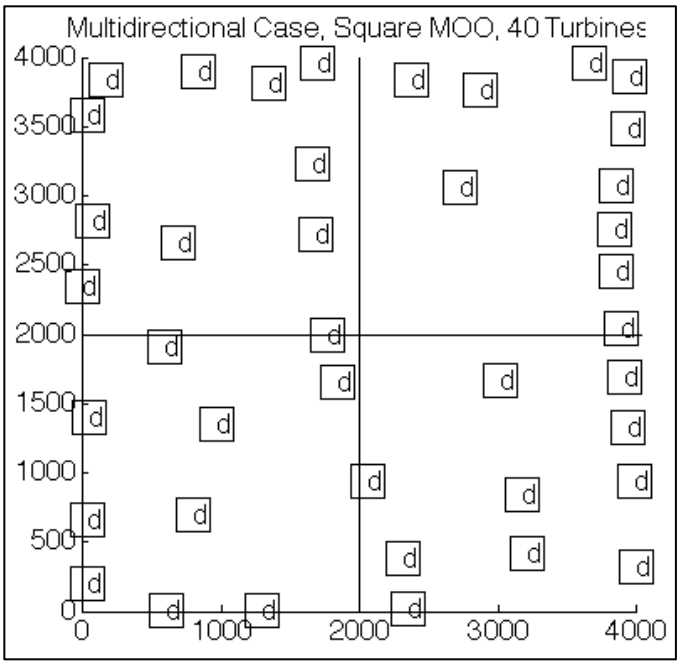

Figure 20: MULTIDIRECTIONAL CASE, MULTI-OBJECTIVE OPTIMIZATION OVER SEQUENTIAL LAND, SQUARE CASE, 40 TURBINES

CONCLUDING DISCUSSION

The purpose of this work was to explore wind farm layout optimization in stages, and discern any relevant insight that can be applied to real-world wind farm stage optimization in the future. Though the means by which multi-stage farms are designed are not made public, it is important to understand whether the current prevalence of a) straight lines of turbines perpendicular to a predominant wind direction, with a large downstream distance to any subsequent rows, and b) the use of new, adjacent land to build subsequent sub-farms are truly optimal solutions.

The first EPS method employed, the full-farm optimization and secondary micro-GA post layout sub-farm identification explored what is postulated to be a directive amongst wind farm developers – to create an optimal final layout without necessarily focusing on the optimality of the sub-farms. The results here were particularly interesting in a few ways. For both the unidirectional and multidirectional cases, the first sub-farm - including only the first stage of ten turbines (Figures 14 and 19) - exhibit "hollowed-out" behavior that has been evident in previous wind farm optimization work [7]. That is, the turbines attempt to maximize the downstream distance between them. For the unidirectional case, this corresponds to turbines moving toward the very front and very back of the field; and for the multidirectional case, migration toward the outer edges of the field. As more turbines are added to the space, the field fills in, with turbines generally avoiding placement in straight lines, (to avoid wake interaction). The 10-turbine sub-farm results from the square case is interesting to note, due to the fact that this smallest sub-farm is essentially two straight lines of turbines across the front and back of the field. This result is commonly seen on some larger wind farms, like the aforementioned Horse Hollow Wind Energy Center in Texas – multiple straight lines of turbines that are oriented perpendicular to the prevailing oncoming wind direction. This layout suggests that this turbine placement method is acceptable given there is significant downstream distance (in this case, 4km) for the wind speed within the wake to recover. Additionally, the turbines that are performing the least optimally - either having smaller geometries that don't generate as much power, or were upstream of many other turbines – are generally removed from the layouts first and saved for the last stage.

The second EPS method, the weighted multi-objective optimization over sequential, adjacent land, is meant to constrain the layouts of each stage to mimic the addition of stages on adjacent plots of land. Based on the plots identified in Figure 6, 10 turbines are placed in each of four stages to create 3 subsequent sub-farms and one final, complete farm. Similar to the results of the full-farm optimization, there is some clustering at the front and back of the square field for the unidirectional case (Figure 15), and the multidirectional layout exhibits some migration toward the outside perimeter of the field (Figure 20). Results from the multidirectional multi-objective layout are particularly interesting to note, as each turbine has selected the largest turbine geometry possible given the defined size constraints. This indicates that the additional cost needed to purchase, install, and service these larger turbines is offset by their higher power development, leading to an increase in profit.

In general, there are a few insights gained from this optimization that can be translated to wind farm development. For a multi-stage farm, the multi-objective optimization was able to develop a layout with significantly higher profit than the full-farm optimization (for the more real-world applicable multidirectional case). This suggests that while the optimality of the full farm is vital, the performance of each sub-farm leading to the final farm's completion must also be considered. This effect is less clear for a farm with a single, predominant wind direction. Additionally, the effect of enabling the turbines to capitalize on a greater wind resource at higher altitudes (evidenced by the selection of larger turbine geometries) and greater wind speeds within wakes (evidenced by maximizing the downstream distance between turbines) is clearly noted for each of the multi-stage examples, implying the importance of employing these insights in real-world multi-stage farm development. In this work, results for a square field were presented. A rectangular field has also been analyzed, although the results are beyond the scope of this paper; the rectangular field design and its results and comparison to the square field will be presented in a future publication.

ACKNOWLEDGEMENTS

This work was funded in part by the National Science Foundation under grants CMMI-0940730 and CMMI-0855326. The authors would like to thank Jason Fields, Andrew Clifton and Levent Burak Kara for discussions and suggestions for this work

REFERENCES

[1] United States Department of Energy, 2008, 20% Wind by 2030, http://www.nrel.gov/docs/fy08osti/41869.pdf.

[2] Wiser R., and Bolinger M., 2012, 2011 Wind Technologies Market Report.

[3] Association A. W. E., 2012, AWEA Third Quarter 2012 Market Report.

[4] "Terra-Gen Power, LLC.," http://www.terra-genpower.com/Projects/Projects_Wind.aspx.

[5] "E.ON Climate and Renewables Roscoe Wind Energy Complex," http://eoncrna.com/contentProjectsRoscoe.html.

[6] 2006, "Horse Hollow I , II & III Wind Energy Center," Resources, Next Era Energy, p. 213 [Online]. Available: http://www.nexteraenergyresources.com/content/where/portfolio/pdf/horsehollow.pdf.

 Copyright © 2013 by ASME

Downloaded From: http://proceedings.asmedigitalcollection.asme.org/ on 03/27/2015 Terms of Use: http://asme.org/terms

[7] DuPont B. L., and Cagan J., 2012, "An Extended Pattern Search Approach to Wind Farm Layout Optimization," ASME Journal of Mechanical Design, **134**, pp. 1–18.
[8] Manwell J. F., McGowan J. G., and Rogers A. L., 2009, Wind Energy Explained: Theory, Design and Application, John Wiley and Sons, Chichester, UK.
[9] Mosetti G., Poloni C., and Diviacco B., 1994, "Optimization of wind turbine positioning in large windfarms by means of a genetic algorithm," Journal of Wind Engineering and Industrial Aerodynamics, **51**(1), pp. 105–116.
[10] Jensen N. O., 1983, A Note on Wind Generator Interaction, Riso National Laboratory, Roskilde, Denmark.
[11] Grady S. A., Hussaini M. Y., and Abdullah M. M., 2005, "Placement of wind turbines using genetic algorithms," Renewable Energy, **30**(2), pp. 259–270.
[12] Elkington C. N., Manwell J. F., and McGowan J. G., 2005, "Offshore Wind Farm Layout Optimization (OWFLO) Project: An Introduction," Optimization.
[13] Elkinton C. N., Manwell J. F., and Mcgowan J. G., "Offshore Wind Farm Layout Optimization (OWFLO) Project : Preliminary Results," AIAA, pp. 1–9.
[14] Wan C., Wang J., Yang G., Li X., and Zhang X., 2009, "Optimal micro-siting of wind turbines by genetic algorithms based on improved wind and turbine models," Proceedings of the 48h IEEE Conference on Decision and Control (CDC) held jointly with 2009 28th Chinese Control Conference, (3), pp. 5092–5096.
[15] Wang F., Liu D., and Zeng L., 2009, "Study on computational grids in placement of wind turbines using genetic algorithm," 2009 World Non-Grid-Connected Wind Power and Energy Conference, **2**, pp. 1–4.
[16] Wang F., Liu D., and Zeng L., 2009, "Modeling and simulation of optimal wind turbine configurations in wind farms," 2009 World Non-Grid-Connected Wind Power and Energy Conference, pp. 1–5.
[17] Huang H. S., 2007, "Distributed Genetic Algorithm for Optimization of Wind Farm Annual Profits," 2007 International Conference on Intelligent Systems Applications to Power Systems, pp. 1–6.
[18] Huang H. S., 2009, "Efficient hybrid distributed genetic algorithms for wind turbine positioning in large wind farms," 2009 IEEE International Symposium on Industrial Electronics, (ISIE), pp. 2196–2201.
[19] Sisbot S., Turgut O., Tunc M., and Camdali U., 2009, "Optimal Positioning of Wind Turbines on Gokceada Using Multi-Objective Genetic Algorithm," Wind Energy, **13**(4), pp. 297–306.
[20] Emami A., and Noghreh P., 2010, "New approach on optimization in placement of wind turbines within wind farm by genetic algorithms," Renewable Energy, **35**(7), pp. 1559–1564.
[21] Rasuo B., and Bengin A., 2010, "Optimization of Wind Farm Layout," pp. 107–114.
[22] Aytun Ozturk U., and Norman B. A., 2004, "Heuristic methods for wind energy conversion system positioning," Electric Power Systems Research, **70**(3), pp. 179–185.
[23] Bilbao M., and Alba E., 2009, "Simulated Annealing for Optimization of Wind Farm Annual Profit," 2009 2nd International Symposium on Logistics and Industrial Informatics, Ieee, Linz, Australia, pp. 1–5.
[24] Mustakerov I., and Borissova D., 2010, "Wind turbines type and number choice using combinatorial optimization," Renewable Energy, **35**(9), pp. 1887–1894.
[25] Wan C., Wang J., Yang G., and Zhang X., 2010, "Optimal Micro-siting of Wind Farms by Particle Swarm Optimization," ICSI 2010, pp. 198–205.
[26] DuPont B. L., Cagan J., and Moriarty P., 2012, "Optimization of Wind Farm Layout and Wind Turbine Geometry Using A Multi-Level Extended Pattern Search Algorithm that Accounts for Changes in Wake Profile Shape," ASME IDETC, Chicago, Illinois, USA.
[27] Zhang J., Chowdhury S., Messac A., Castillo L., and Lebron J., 2010, "Response Surface Based Cost Model for Onshore Wind Farms Using Extended Radial Basis Functions," ASME Internation Design Engineering Technical Conference, Montreal, QC, Canada, pp. 1–16.
[28] Chowdhury S., Messac A., Zhang J., Castillo L., and Lebron J., 2010, "Optimizing the Unrestricted Placement of Turbines of Differing Rotor Diameters in a Wind Farm for Maximum Power Generation," ASME IDETC, Montreal, QC, Canada, pp. 1–16.
[29] Benatiallah A., and Dakyo B., 2010, "Modelling and Optimisation of Wind Energy Systems," Jordan Journal of Mechanical and Industrial Engineering, **4**(1), pp. 143–150.
[30] Chen L., and Macdonald E., 2011, "A New Model for Wind Farm Layout Optimization with Landowner Decisions," ASME International Design Engineering Technical Conference, pp. 1–12.
[31] Kusiak A., and Zheng H., 2010, "Optimization of wind turbine energy and power factor with an evolutionary computation algorithm," Energy, **35**(3), pp. 1324–1332.
[32] Chowdhury S., Zhang J., Messac A., and Castillo L., 2013, "Optimizing the arrangement and the selection of turbines for wind farms subject to varying wind conditions," Renewable Energy, **52**, pp. 273–282.
[33] "Oregon Department of Energy Stateline Wind Project," 2010 [Online]. Available: http://www.oregon.gov/ENERGY/SITING/Pages/SWP.aspx.
[34] Yin S., and Cagan J., 2000, "An Extended Pattern Search Algorithm for Three-Dimensional Component Layout," ASME Journal of Mechanical Design, **122**, pp. 102–108.
[35] Talukdar S., Baerentzen L., Gove A., and Souza P. De, 1996, "Asynchronous Teams: Cooperation Schemes for Autonomous Agents," Journal of Heuristics, **4**, pp. 295–321.
[36] Campbell M. I., Cagan J., and Kotovsky K., 1999, "A-Design- An Agent-Based Approach to Conceptual Design in a Dynamic Environment," Research in Engineering Design, **11**, pp. 172–192.
[37] Nii H. P., 1986, "Blackboard Application Systems and a Knowledge Engineering Perspective," AI Magazine, pp. 82–107.
[38] Rohatgi J., and Barbezier G. I. L., 1999, "Wind Turbulence and Atmospheric Stability - Their Effect on Wind Turbine Output," Renewable Energy, **16**, pp. 908–911.
[39] Hiester T. R., and Pennell W. T., 1981, The Meteorological Aspects of Siting Large Wind Turbines, US Dept. of Energy.
[40] Frandsen S., Antoniou I., Hansen J. C., Kristensen L., Chaviaropoulos B., Douvikas D., Dahlberg J. A., Derrick A., Dunbabin P., Hunter R., Ruffle R., Kanellopoulos D., and Kapsalis G., 2000, "Redefinition Power Curve for More Accurate Performance Assessment of Wind Farms," Wind Energy, **3**, pp. 81–111.

 Copyright © 2013 by ASME

Downloaded From: http://proceedings.asmedigitalcollection.asme.org/ on 03/27/2015 Terms of Use: http://asme.org/terms

[41] Sumner J., and Masson C., 2006, "Influence of Atmospheric Stability on Wind Turbine Power Performance Curves," Journal of Solar Energy Engineering, **128**(4), p. 531.
[42] Kelley N., Shirazi M., Jager D., Wilde S., Adams J., Buhl M., Sullivan P., and Patton E., 2004, Lamar Low-Level Jet Project Interim Report, Golden, CO.
[43] Larsen S., Ott S., Peña A., Berg J., Nielsen M., Rathmann O., and Jørgensen H., 2011, Wake models developed during the Wind Shadow Project Risø-R-Report, Roskilde, Denmark.
[44] Pena A., and Rathmann O., 2011, The Atmospheric Stability Dependent Infinite Wind Farm and Wake Decay Coefficient, Roskilde, Denmark.
[45] Alblas L. M., 2012, "Power Output of Offshore Wind Farms in Relation to Atmospheric Stability," Delft University of Technology.
[46] Barthelmie R. J., and Jensen L. E., 2010, "Evaluation of wind farm efficiency and wind turbine wakes at the Nysted offshore wind farm," Wind Energy, **13**(June), pp. 573–586.
[47] Katic I., Hojstrup J., and Jensen N. O., 1986, "A Simple Model for Cluster Efficiency," European Wind Energy Association Conference and Exhibition, Rome, Italy, pp. 407–410.
[48] Fingersh L., Hand M., and Laxson A., 2006, Wind Turbine Design Cost and Scaling Model, National Renewable Energy Laboratory, Golden, CO.
[49] NREL, "NREL JEDI Models," http://www.nrel.gov/analysis/jedi/download.html [Online]. Available: http://www.nrel.gov/analysis/jedi/download.html.
[50] Senecal P. K., 2000, "NUMERICAL OPTIMIZATION USING THE GEN4 MICRO- GENETIC ALGORITHM CODE," University of Wisconsin-Madison.

 Copyright © 2013 by ASME

Downloaded From: http://proceedings.asmedigitalcollection.asme.org/ on 03/27/2015 Terms of Use: http://asme.org/terms